Mathematical Biosciences and Engineering

http://www.aimspress.com/journal/mbe

MBE, 20(2): 4219–4242.
DOI: 10.3934/mbe.2023197
Received: 17 October 2022
Revised: 18 November 2022
Accepted: 04 December 2022
Published: 21 December 2022

Research article

Stochastic sensitivity analysis and feedback control of noise-induced transitions in a predator-prey model with anti-predator behavior

Mengya Huang[1], **Anji Yang**[1], **Sanling Yuan**[1,*] **and Tonghua Zhang**[2]

[1] College of Science, University of Shanghai for Science and Technology, Shanghai 200093, China
[2] Department of Mathematics, Swinburne University of Technology, Hawthorn, VIC 3122, Australia

* **Correspondence:** Email: sanling@usst.edu.cn.

Abstract: In this study, we investigate a stochastic predator-prey model with anti-predator behavior. We first analyze the noise-induced transition from a coexistence state to the prey-only equilibrium by using the stochastic sensitive function technique. The critical noise intensity for the occurrence of state switching is estimated by constructing confidence ellipses and confidence bands, respectively, for the coexistence the equilibrium and limit cycle. We then study how to suppress the noise-induced transition by using two different feedback control methods to stabilize the biomass at the attraction region of the coexistence equilibrium and the coexistence limit cycle, respectively. Our research indicates that compared with the prey population, the predators appear more vulnerable and prone to extinction in the presence of environmental noise, but it can be prevented by taking some appropriate feedback control strategies.

Keywords: predator-prey model; anti-predator behavior; noise-induced state switching; critical noise intensity; feedback control

1. Introduction

In a population system, when a population preys on another population in order to survive, the preyed species will have a sense of self-protective, and this self-protective behavior is called anti-predation behavior. Species use a variety of methods to protect themselves, such as camouflage, avoiding confrontation, changing body color and releasing toxins in the form of chemical defense, and different species tend to protect themselves by using different methods [1]. But anti-predation behavior not only refers to prey attacking relatively weak predators, as it also includes prey killing stronger predators together, such as the phenomenon of herd defense, which occors when the prey is in sufficient numbers, the ability of the prey to better defend or camouflage itself increases, leading to reduced or even completely blocked predation [2–4]. For instance, Huang et al. [5] mentioned that

when the prey species are spider mites, a possible source of disturbance is the web produced by these mites, which reduces the predator's walking speed and chances of catching prey. Therefore, predators not adapted to walking on the web may also starve to death in the presence of spider mites.

Using mathematical language to describe the relationship between predator and prey can provide a theoretical basis for problems encountered in real world. The interactions between biological populations are often characterized by functional response functions. In the predator-prey model, the intensity of the functional response of predators to prey is critical, as it enriches the dynamics of the predator-prey system [6]. Many researchers have investigated predator-prey models with the Holling type IV functional response function [7–10]. For example, Ruan and Xiao [8] studied the global dynamics of a predator-prey model with such a non-monotonic functional response function and proved that saddle-node bifurcation, Hopf bifurcation and B-T bifurcation would occur. Based on [8], Tang and Xiao [11] considered the influence of anti-predator behavior and proposed the following model with the Holling type IV functional response function:

$$\begin{cases} \dfrac{\mathrm{d}x}{\mathrm{d}t} = rx\left(1 - \dfrac{x}{k}\right) - \dfrac{\beta xy}{a + x^2}, \\ \dfrac{\mathrm{d}y}{\mathrm{d}t} = \dfrac{\mu\beta xy}{a + x^2} - dy - \eta xy, \end{cases} \tag{1.1}$$

where all parameters are positive. r is the intrinsic growth rate of the prey. k is the environmental capacity. β is the capture rate of the predator. μ is the rate of conversion of prey to predator. d is the natural death rate of the predator population. η is the anti-predator behavior rate of the prey in response to the predator population. It is worth emphasizing that most works describe anti-predator behavior only through functional response functions, whereas the model (1.1) not only describes the phenomenon that the predation rate decreases with increasing prey density through the Holling IV functional response function, but it also characterizes the phenomenon that adult prey can kill weak predators. In [11], Tang and Xiao analyzed the existence and stability of all possible equilibria of the predator-prey model (1.1) with anti-predator behavior, and they conducted a detailed and complete bifurcation analysis, including saddle-node bifurcation, Hopf bifurcation, homoclinic bifurcation and B-T bifurcation of codimension 2.

The results of the deterministic model can indeed provide us with some theoretical reference, but the dynamics of the deterministic model depends closely on the initial value and model parameters, which are extremely sensitive to environmental fluctuations [12–14]. Obviously, the establishment of deterministic models is based on several identified populations, consistent patterns of behavior, and specific environments [15]. But real life is full of randomness and unpredictability. A series of biological and environmental factors in the ecosystem will cause population fluctuations, and environmental uncertainty, which is influenced by factors such as the temperature, the climate, and rainfall will lead to noise [16]. Fluctuations of the environment can even dramatically change the dynamic behavior of the model [17]. For example, Bawa et al. [18] experimentally demonstrated that extreme temperatures negatively affected Helicoverpa punctigera pupae. It was found that the application of heat stress to pupae could affect Helicoverpa punctigera population dynamics by reducing fecundity and prolonging pre-oviposition and affecting adult development. Due to heat exposure, the parent did not produce offspring. Therefore, in order to accurately characterize the impact of environmental fluctuations, many scholars have carried out a series of studies by incorporating stochastic factors into deterministic models [19–24]. For instance, Liu et al. [23]

studied a state-transition predator-prey model with anti-predator behavior and higher-order perturbations, and they obtained the ergodic property by constructing a suitable stochastic Lyapunov function. Zhang et al. [24] proposed a stochastic predator-prey model with habitat complexity and prey aggregation efficiency, proved the existence, uniqueness and stochastic uniformity of the global positive solution of the model, and found sufficient conditions for the existence of ergodic stationary distributions. It is worth emphasizing that most of the existing literature on stochastic predator-prey models mainly pay attention to the long-term qualitative behavior of the model and the existence of an ergodic stationary distribution, while our work in this paper provides a quantitative analysis of how noise affects the system.

The research on the impact of environmental noise on the system has also attracted the attention of many scholars [25–28]. For example, Zhou et al. [25] studied stationary distribution, extinction and probability density functions for stochastic vegetation-water models in arid ecosystems, verified the theoretical results through numerical simulation based on the data and studied the impact of random noise on vegetation dynamics. Bashkirtseva et al. [29] proposed a novel method based on the stochastic sensitivity function technique to construct an analytical description of the stochastic forced equilibrium and loops of discrete-time models. Further, Yuan et al. [30] used the stochastic sensitivity function technique to analyze the noise-induced state transition phenomenon in a non-smooth producer-grazer model with stoichiometric constraints. They found that stochastic trajectories jump frequently between two stochastic attractors. From a biological point of view, people often prefer species to maintain a high biomass state to enrich the diversity and stability of ecosystems. Therefore, it is necessary to control the sensitivity of the ecosystem to environmental noise. In order to suppress the stochastic sensitivity of equilibrium points and limit cycles, Ryashko and Bashkirtseva [31, 32] proposed control principles of stochastic sensitivity for equilibrium points and limit cycles respectively, and carried out numerical simulations with examples. In this study, we used the stochastic sensitivity function technique to respectively construct the corresponding confidence ellipses and confidence bands for equilibrium points and limit cycles, and then estimated the critical noise intensity at the noise-induced system state transitions. Next, different control methods were applied to stabilize the biomass at the attraction region of the coexistence equilibrium point and the coexistence limit cycle, respectively.

The rest of this paper is structured as follows. We outline the main results of the deterministic model (1.1) and formulate the corresponding stochastic predator-prey model with anti-predator behavior in Section 2. In Section 3, we analyze the state transitions between the equilibrium point and the equilibrium point (or the limit cycle and the equilibrium point) induced by noise; we also estimate the critical thresholds for state transitions by using confidence ellipses and confidence bands, respectively. According to the feedback control principle, we control the sensitivity between the two equilibrium points (or the limit cycle and the equilibrium point) in Section 4. Finally, we give a brief summary of this paper in Section 5 to conclude our study.

2. Model formulation

2.1. Restate the main results of the deterministic model

We briefly revisit some results from [11]: the system (1.1) has two boundary equilibria $E_0 = (0, 0)$ and $E_k = (k, 0)$, and up to two coexisting equilibrium points $E_i = (x_i, y_i)$, $i = 1, 2$, where

$$x_1 = \frac{-d + \sqrt{A}\left(\cos\frac{\theta}{3} - \sqrt{3}\sin\frac{\theta}{3}\right)}{3\eta}, y_1 = \frac{1}{\beta}r\left(1 - \frac{x_1}{k}\right)(a + x_1^2),$$

$$x_2 = \frac{-d + \sqrt{A}\left(\cos\frac{\theta}{3} + \sqrt{3}\sin\frac{\theta}{3}\right)}{3\eta}, y_2 = \frac{1}{\beta}r\left(1 - \frac{x_2}{k}\right)(a + x_2^2),$$

where $A = d^2 - 3\eta(\eta a - \mu\beta)$, $B = d(\eta a - \mu\beta) - 9\eta ad$, $\theta = \arccos T$ and $T = \dfrac{2Ad - 3\eta B}{2\sqrt{A^3}}$. Further, we have the following lemma.

Lemma 1. *For $k > x_2$, if there is a stable boundary equilibrium point $E_k = (k, 0)$, a stable node E_1, and a saddle point E_2, but E_1 gradually loses its stability as k increases, then a locally stable limit cycle Γ' appears. In other words, the system* (1.1) *has two types of bistability: the coexistence of two stable equilibrium points E_k and E_1 or a stable equilibrium point E_k and a stable Γ'.*

For the purpose of our study, in this paper, we mainly focus on the parameter domains when the system admits bistability. Therefore, we treat the environmental capacity k as a control parameter and fix other parameters of the model as follows:

$$r = 0.05, a = 0.8, \mu = 0.8, \beta = 0.6, \eta = 0.01, d = 0.24. \tag{2.1}$$

In this set of parameters, we take $k = 1.45$, and then system (1.1) has a stable coexistence equilibrium point $E_1 = (0.58509, 0.05678)$, a saddle point $E_2 = (1.26925, 0.02505)$ and a stable boundary equilibrium point $E_3 = (1.45, 0)$, as shown in Figure 1(a). The red dotted line Γ in the figure is the separatrix between two domains of attraction in the first quadrant. The trajectories starting from the interior of the separatrix finally converge to the coexistence equilibrium point E_1, and the trajectories starting from the outside of the separatrix tend to the predator extinction equilibrium point E_3. That is, depending on the initial value, the final population will tend to the coexistence equilibrium E_1 or the predator extinction equilibrium E_3. When $k = 1.6$, as shown in Figure 1(b), the system (1.1) has a stable boundary equilibrium point $E_4 = (1.6, 0)$ and a saddle point E_2. E_1 loses stability resulting in a stable limit cycle Γ'. In this case, the species biomass exhibits a periodic oscillation pattern.

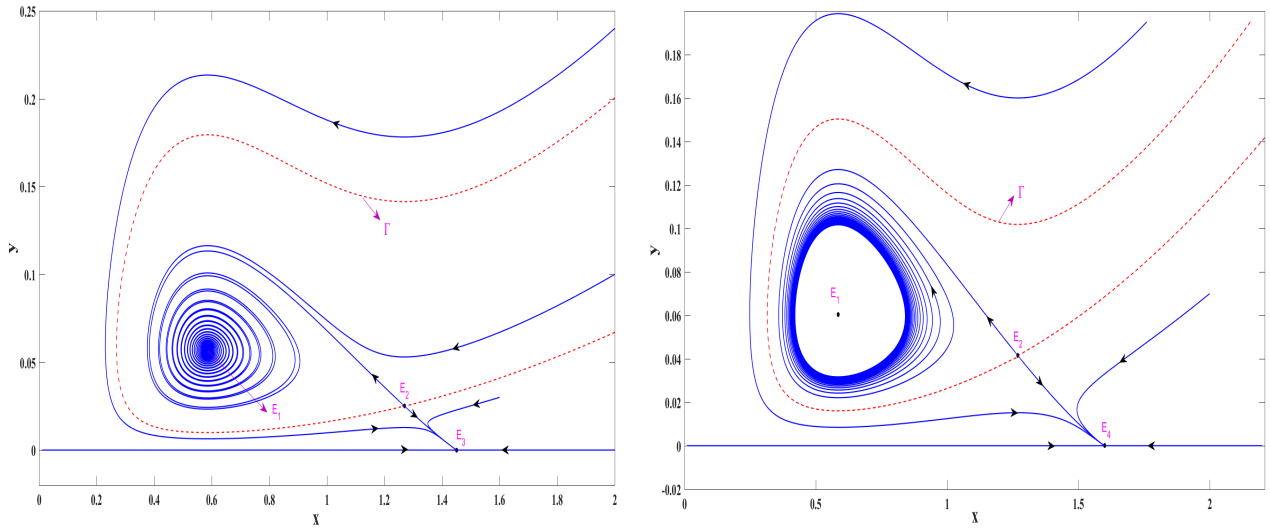

(a) (b)

Figure 1. Phase plane of the system (1.1): (a) parameter settings given (2.1) and $k = 1.45$; (b) parameter settings given (2.1) and $k = 1.6$. Here the red dotted curves Γ are the separatrices between the two domains of attraction, and the blue solid curves are the trajectories of the model with different initial values.

2.2. Stochastic model

Since the deterministic systems are inevitably affected by various environmental noises, which will further affect or even change the original properties of the deterministic model, we use the idea of small perturbation to incorporate the noise into the model. Thus, based on the model (1.1), we consider the following stochastic differential equation

$$\begin{cases} dx = \left(rx\left(1 - \dfrac{x}{k}\right) - \dfrac{\beta xy}{a + x^2}\right)dt + \sigma_1 x dB_1, \\ dy = \left(\dfrac{\mu\beta xy}{a + x^2} - dy - \eta xy\right)dt + \sigma_2 y dB_2, \end{cases} \tag{2.2}$$

where $B_1(t)$ and $B_2(t)$ are independent standard one-dimensional Brownian motions, which are defined in a complete probability space $(\Omega, \{\mathcal{F}_t\}_{t\geq 0}, Prob)$ with a fltration $\{\mathcal{F}_t\}$ satisfying the usual normal conditions (right continuous and increasing while $\mathcal{F}_0$ contains all probability-null sets). σ_1 and σ_2 represent noise intensities. For simplicity, we assume $\sigma_1 = \sigma_2 = \sigma$ in our study. Next, we study the properties of the model (2.2).

3. Analysis of noise-induced transitions

3.1. Sensitivity analysis of noise-induced transitions between attractors

As mentioned earlier, for a deterministic model, the evolution of the solution is completely determined by the initial values and model parameters. But, for stochastic models, the behavior of stochastic trajectories can be very complex and interesting. Next, we will explore the dynamical

behavior of the stochastic model (2.2) in the presence of noise. Take $\sigma = 0.004$ and the initial value $(0.5851, 0.0568)$ near E_1; the trajectory from this initial value will hover around E_1 (see Figure 2).

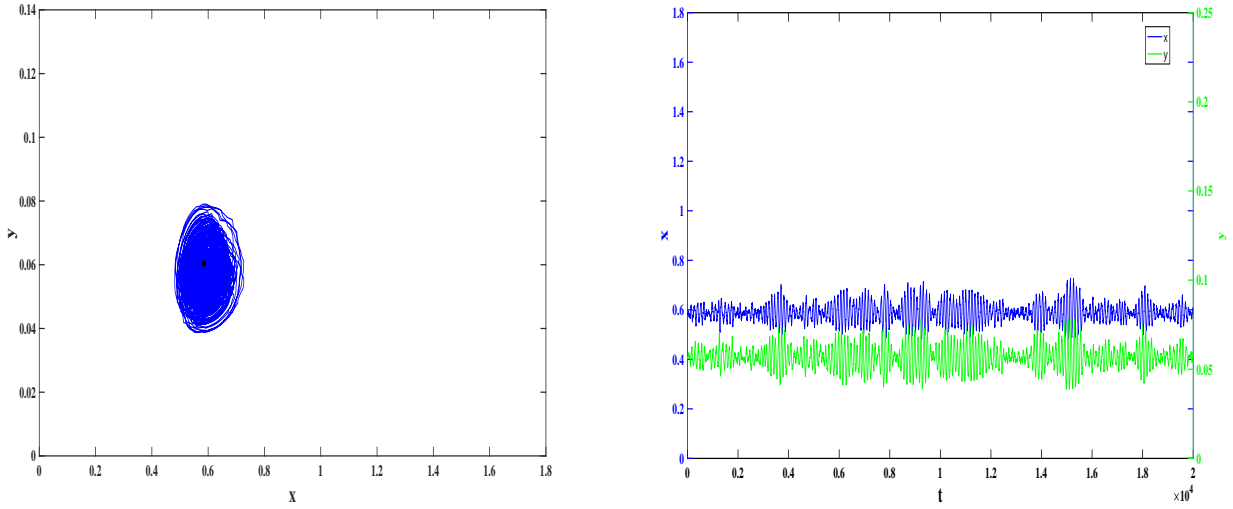

(a) (b)

Figure 2. Random trajetory (a) and time series (b) of the stochastic system (2.2) for $\sigma = 0.004$ with the inital value $(0.5851, 0.0568)$.

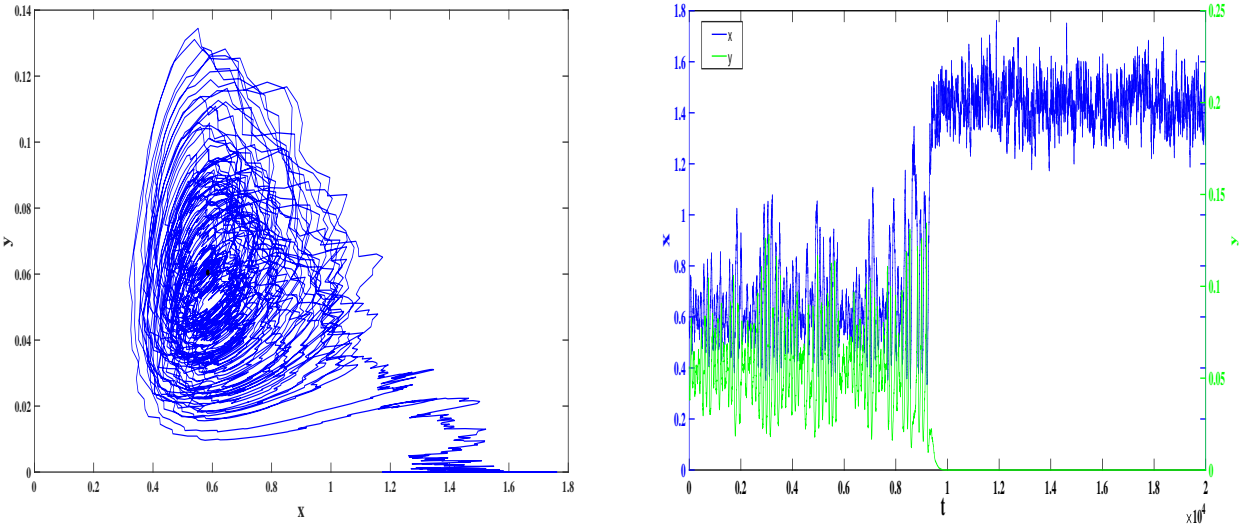

(a) (b)

Figure 3. Random trajetory (a) and time series (b) of the stochastic system (2.2) for $\sigma = 0.0175$ with the inital value $(0.5851, 0.0568)$.

But when the noise intensity gradually increases and becomes large enough, the solution of the stochastic model (2.2) will behave very different from the behavior shown in Figure 2. Here, we take $\sigma = 0.0175$, and the stochastic trajectory escapes from the domain of attraction of E_1 and enters the

domain of attraction of E_3. That is, in this case, the predator biomass tends to extinction while the prey biomass increases significantly (Figure 3). These noise-induced transitions suggest that the coexistence of the two species is disrupted and predators can be forced to extinction.

From the above analysis, it can be seen that the critical noise intensity σ^* of the noise-induced stochastic model (2.2) state transitioning from the coexistence state to the prey-only state is between 0.004 and 0.0175. When $0.004 < \sigma < \sigma^*$, the stochastic model (2.2) has persistence; thus, the predator and prey coexist. To further determine the critical threshold σ^* for noise-induced model state transitions, using the stochastic sensitive function technique in [33], we construct confidence ellipses for the equilibrium point E_1.

For the coexistence equilibrium point $E_1 = (x_1, y_1)$ of the deterministic model (1.1), let $F = \begin{pmatrix} f_{11} & f_{12} \\ f_{21} & f_{22} \end{pmatrix}$ be the Jacobian matrix at $E_1 = (x_1, y_1)$, where

$$\begin{aligned} f_{11} &= r - \frac{2rx}{k} - \frac{\beta y}{a + x^2} + \frac{2\beta x^2 y}{(a + x^2)^2}, \\ f_{12} &= -\frac{\beta x}{a + x^2}, \\ f_{21} &= \frac{\mu\beta y}{a + x^2} - \frac{2\mu\beta x^2 y}{(a + x^2)^2} - \eta y, \\ f_{22} &= \frac{\mu\beta x}{a + x^2} - d - \eta x, \end{aligned}$$

we define $g_{11} = x$, $g_{22} = y$, and $G = \begin{pmatrix} g_{11} & 0 \\ 0 & g_{22} \end{pmatrix}$. After solving the following system of linear equations for w_{ij}, $i, j = 1, 2$,

$$\begin{cases} 2f_{11}w_{11} + f_{12}w_{12} + f_{12}w_{21} = -g_{11}^2, \\ f_{21}w_{11} + (f_{11} + f_{22})w_{12} + f_{12}w_{22} = 0, \\ f_{21}w_{11} + (f_{11} + f_{22})w_{21} + f_{12}w_{22} = 0, \\ f_{21}w_{12} + f_{21}w_{21} + 2f_{22}w_{22} = -g_{22}^2, \end{cases}$$

we get the stochastic sensitive matrix as $W = \begin{pmatrix} w_{11} & w_{12} \\ w_{21} & w_{22} \end{pmatrix}$.

Given a noise intensity σ and fiducial probability P, the confidence ellipse equation at $E_1 = (x_1, y_1)$ can be obtained by applying Formula $A.3$ in [33] as

$$\left\langle (x - x_1, y - y_1)^T, W^{-1}((x - x_1, y - y_1)^T) \right\rangle = 2\sigma^2 \ln \frac{1}{1 - P}. \tag{3.1}$$

Applying the above method to the coexistence equilibrium point $E_1 = (0.58509, 0.05678)$, we respectively obtain the corresponding stochastic sensitivity matrix and its inverse as

$$W = \begin{pmatrix} 98.4026 & -0.1794 \\ -0.1794 & 2.8803 \end{pmatrix} \text{ and } W^{-1} = \begin{pmatrix} 0.0102 & 0.0006 \\ 0.0006 & 0.3472 \end{pmatrix}.$$

The confidence ellipse equation of E_1 is

$$0.0102 \cdot (x - 0.58509)^2 + 0.0012 \cdot (x - 0.58509)(y - 0.05678) + 0.3472 \cdot (y - 0.05678)^2 = 2\sigma^2 \ln \frac{1}{1 - P}.$$

Fixing the fiducial probability at $P = 0.95$, we vary the noise intensity and observe the effect of the noise intensity on the confidence ellipse. The corresponding stochastic states and confidence ellipses of the system (2.2) with $\sigma = 0.00675$ are shown in Figure 4(a). This figure shows that the stochastic states are distributed around the deterministic equilibrium point E_1 and have a probability of 0.95 of lying inside the confidence ellipse.

Next, we select different noise levels $\sigma = 0.0085$, 0.0113 and 0.0135, which respectively correspond to the small, medium and large confidence ellipses of the solid blue line in Figure 4(b). Obviously, with the continuous increase of the noise intensity, the confidence ellipse continues to increase and exceeds the separatrix Γ of the two attraction domains; it contains the domain of attraction of the partial predator extinction equilibrium point E_3. When the confidence ellipse is tangent to the separatrix Γ, the corresponding noise intensity is the estimated value of the critical noise σ^* of the noise-induced stochastic model state transition, where $\sigma^* \approx 0.0113$. In Figure 3, a typical example is that the trajectory of the system (2.2) starting near the coexistence equilibrium E_1 converges to the prey-only equilibrium E_3 with $\sigma = 0.0175 > \sigma^*$.

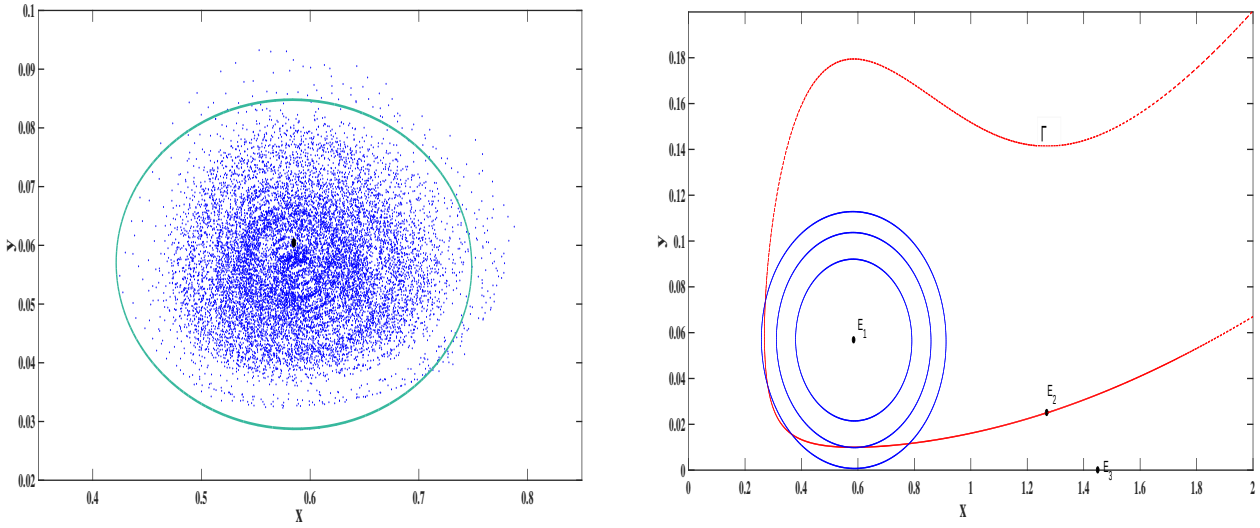

(a) (b)

Figure 4. Random states and confidence ellipses for stochastic system (2.2) with $k = 1.45$. (a) Random states (blue) and equilbrium E_1 (black) of the stochastic model (2.2) and confidence ellipse (green) for $\sigma = 0.00675$. (b) Separatrix (red), equilbrium E_1(black) and confidence ellipse (blue) for $\sigma = 0.0085$ (small), $\sigma = 0.0113$ (middle) and $\sigma = 0.0135$ (large).

3.2. Sensitivity analysis of noise-induced transitions between the limit cycle and equilibrium point

Similarly, we explore another dynamical behavior of the stochastic model (2.2) in the presence of noise. Take $\sigma = 0.004$ and the initial value $(0.5851, 0.0378)$ near the limit cycle Γ'; the trajectory from this initial value will hover around the limit cycle (Figure 5).

But, when the noise intensity gradually increases and becomes large enough, the solution of the stochastic model (2.2) will behave very differently from the behavior shown in Figure 5. Here, we take

$\sigma = 0.03$; the stochastic trajectory escapes from the domain of attraction of Γ' and enters the domain of attraction of E_4. In this case the predator biomass tends to extinction, while the prey biomass increases significantly (Figure 6). That is, the model (2.2) undergoes a state transition and finally converges to the prey-only equilibrium point E_4.

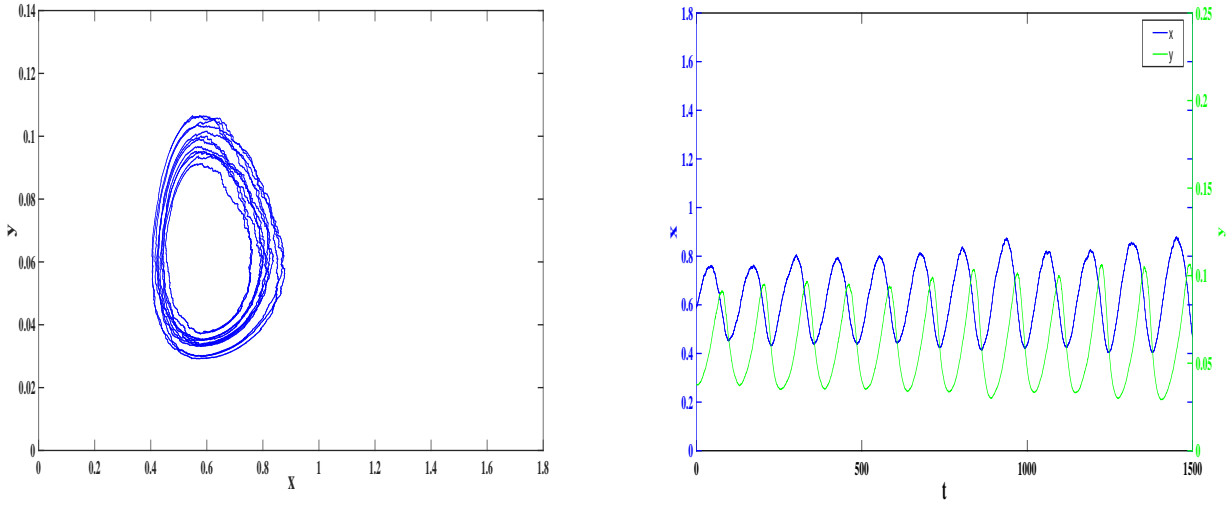

(a) (b)

Figure 5. Random trajetory (a) and time series (b) of the stochastic system (2.2) for $\sigma = 0.004$ with the inital value $(0.5851, 0.0378)$.

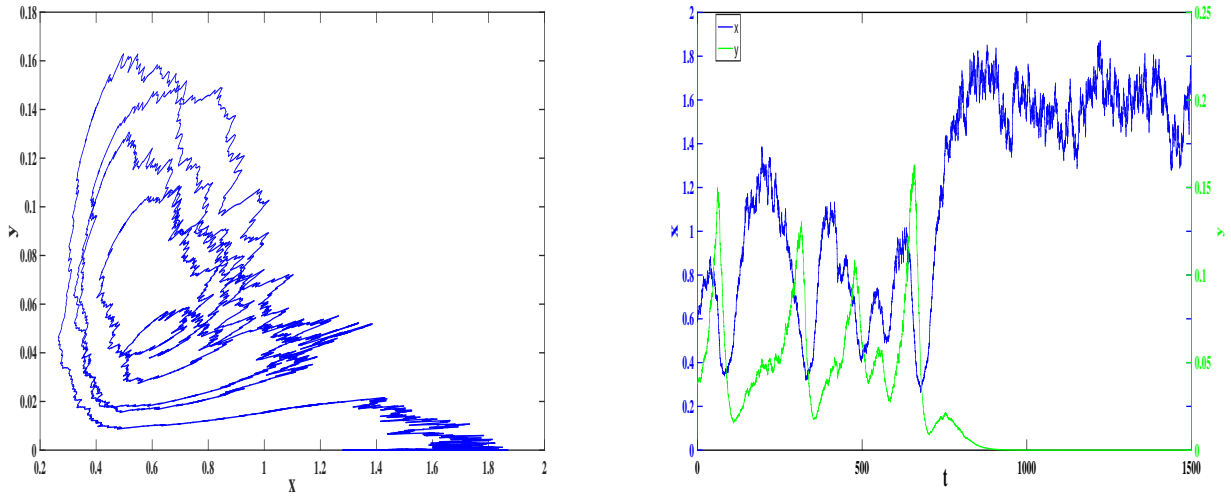

(a) (b)

Figure 6. Random trajetory (a) and time series (b) of the stochastic system (2.2) for $\sigma = 0.03$ with the inital value $(0.5851, 0.0378)$.

From the above analysis, it can be seen that the critical noise intensity σ' of the noise-induced

stochastic model (2.2) transitioning from the coexistence state to the prey-only state is between 0.004 and 0.03. When $0.004 < \sigma < \sigma^{'}$, the stochastic model (2.2) exhibits persistence, which means that the predator and prey coexist. To further determine the critical threshold $\sigma^{'}$ for noise-induced model state transitions, using the stochastic sensitive function technique in [33], we construct corresponding confidence bands for the stochastic system (2.2).

For ease of calculation, define

$$F_1(x,y) = rx\Big(1 - \frac{x}{k} - \frac{\beta xy}{a+x^2}\Big),$$
$$F_2(x,y) = \frac{\mu\beta xy}{a+x^2} - dy - \eta xy.$$

Let $\Gamma^{'}(x(t), y(t))$, $t \in [0, T]$, where T is the period, and denote the limit cycle of a deterministic model. According to the principle of confidence bands in [33], we can write

$$F(t) = \begin{pmatrix} f_{11}(t) & f_{12}(t) \\ f_{21}(t) & f_{22}(t) \end{pmatrix}, G(t) = \begin{pmatrix} g_{11}(t) & 0 \\ 0 & g_{22}(t) \end{pmatrix}, S(t) = G(t)G(t)^T,$$

where

$$f_{11}(t) = \Big(r - \frac{2rx}{k} - \frac{\beta y}{a+x^2} + \frac{2\beta x^2 y}{(a+x^2)^2}\Big)\Big|_{\Gamma'},$$
$$f_{12}(t) = \Big(-\frac{\beta x}{a+x^2}\Big)\Big|_{\Gamma'},$$
$$f_{21}(t) = \Big(\frac{\mu\beta y}{a+x^2} - \frac{2\mu\beta x^2 y}{(a+x^2)^2} - \eta y\Big)\Big|_{\Gamma'},$$
$$f_{22}(t) = \Big(\frac{\mu\beta x}{a+x^2} - d - \eta x\Big)\Big|_{\Gamma'},$$
$$g_{11}(t) = x|_{\Gamma'},$$
$$g_{22}(t) = y|_{\Gamma'}.$$

We know that the random sensitive function $\mu(t)$ satisfies the following boundary value problem [33]:

$$\dot{\mu} = a(t)\mu + b(t), \mu(0) = \mu(T),$$

where

$$a(t) = 2f_{11}(t)p_1^2(t) + 2(f_{12}(t) + f_{21}(t))p_1(t)p_2(t) + 2f_{22}(t)p_2^2(t),$$
$$b(t) = g_{11}(t)p_1^2(t) + g_{22}(t)p_2^2(t).$$

Here,

$$p_1(t) = \frac{F_2(x,y)}{\sqrt{F_1^2(x,y) + F_2^2(x,y)}}\Big|_{\Gamma'},$$
$$p_2(t) = -\frac{F_1(x,y)}{\sqrt{F_1^2(x,y) + F_2^2(x,y)}}\Big|_{\Gamma'},$$

are the components of the vector function $p(t) = (p_1(t), p_2(t))^T$ orthogonal to the vector $(F_1(x,y), F_2(x,y))^T$. According to $A.5$ in [33], the boundary $\Gamma_{1,2}^{'}(t)$ of the confidence band can be

obtained as

$$\Gamma_1^{'}(t) = \Gamma^{'}(t) + \sigma k\sqrt{2\mu(t)}p(t),$$
$$\Gamma_2^{'}(t) = \Gamma^{'}(t) - \sigma k\sqrt{2\mu(t)}p(t),$$

where the parameter $k = erf^{-1}(P)$, P is the fiducial probability, and $erf(x) = \frac{2}{\sqrt{\pi}}\int_0^x e^{-t^2}dt$ is the error function.

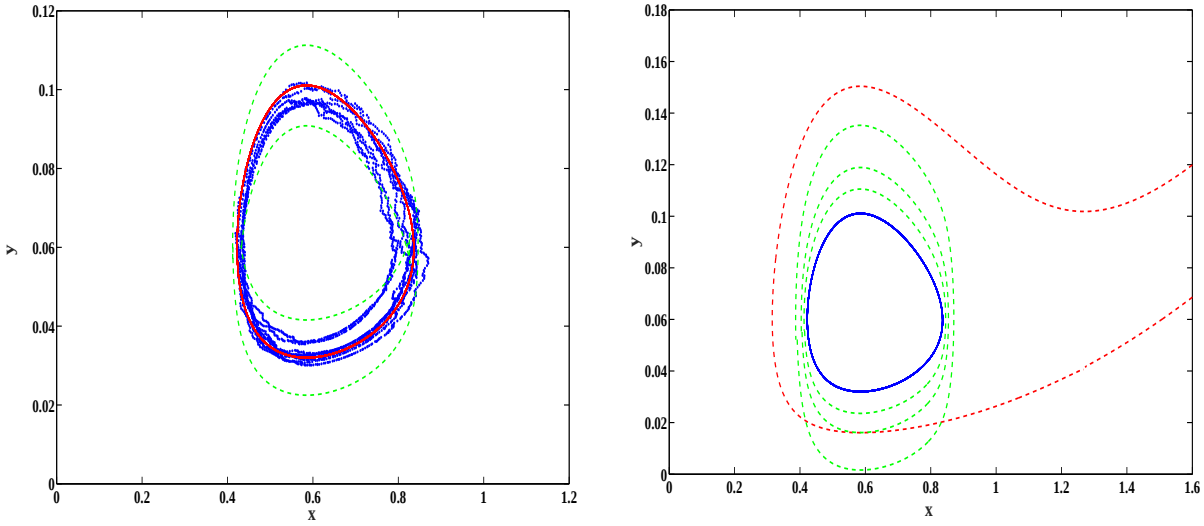

(a) (b)

Figure 7. Random states and confidence bands for stochastic system (2.2) with $k = 1.6$. (a) Random states (blue) of the stochastic model (2.2) around $\Gamma^{'}$ (red) and the confidence band (green) for $\sigma = 0.004$. (b) Separatrix (red dashed), limit cycie $\Gamma^{'}$ (blue) and outer boundary (green dashed) of the confidence belt for $\sigma = 0.005$ (small), $\sigma = 0.0094$ (middle) and $\sigma = 0.018$ (large).

In Figure 7(a), $\sigma = 0.004$, $P = 0.95$, the red line is the deterministic limit cycle $\Gamma^{'}$, the blue points are the stochastic state of the stochastic model (2.2) and the two green dotted lines are the boundaries of the confidence band. Obviously, the stochastic state oscillates around the deterministic limit cycle $\Gamma^{'}$, and their probability within the confidence band interval is 0.95.

In fact, judging whether the model has a state transition only requires attention to the outer boundary of the confidence band. As shown in Figure 7(b), the blue solid line is the deterministic limit cycle $\Gamma^{'}$, the red dashed line is the separatrix between the domains of attraction of the limit cycle $\Gamma^{'}$ and the predator extinction equilibrium point E_4 and the green dashed lines are the outer boundaries of the confidence band corresponding to $\sigma = 0.005$ (small), $\sigma = 0.0094$ (middle) and $\sigma = 0.018$ (large) with $P = 0.95$. It can be seen in the Figure 7(b) that, with the continuous increase of noise intensity, the outer boundary of the confidence band continues to increase to exceed the separatrix Γ of the two attractive domains, and it contains the domain of attraction of the partial predator extinction equilibrium point E_4. When the outer boundary of the confidence band is tangent to the separatrix Γ, the corresponding noise intensity is the estimated value $\sigma^{'}$ of the critical noise of noise-induced transitions from coexistence limit cycles to the extinction equilibrium point. Here $\sigma^{'} \approx 0.0094$. The case of $\sigma = 0.03 > \sigma^{'}$ in

Figure 6 validates our conclusion.

4. Feedback control of noise-induced system from coexistence to extinction

After the analysis in Section 3, we find that there are two situations in which predator extinction occurs. As shown in Figure 3, when the noise intensity $\sigma = 0.0175$, the trajectory of the uncontrolled system (2.2) will escape from the attraction domain of the coexistence equilibrium point E_1, and eventually converge to the prey-only equilibrium point E_3. And, in Figure 6, when the noise intensity $\sigma = 0.03$, the trajectory of the uncontrolled stochastic model (2.2) starting from the attraction domain of the coexistence limit cycle Γ' will also pass through the separatrix of the two attraction domains, eventually tending toward the predator extinction equilibrium point E_4. But from a biological point of view, people often prefer species to maintain a high biomass state to enrich the diversity and stability of ecosystems. Therefore, we will study the sensitivity control problem of the equilibrium point or limit cycle next.

4.1. Sensitivity control of the coexistence equilibrium point

From the analysis in Section 3.1, it can be seen that the critical threshold for the state transition of the noise-induced system from the coexistence equilibrium point E_1 to the predator extinction equilibrium point E_3 is $\sigma^* \approx 0.0113$. When $\sigma = 0.0175 > \sigma^*$, the trajectory starting from the vicinity of the equilibrium point E_1 finally converges to the prey-only equilibrium point E_3. In order to avoid the noise-induced state transition of the population from the coexistence equilibrium point E_1 to the predator extinction equilibrium point E_3, we introduce a feedback control strategy to make the corresponding confidence ellipse smaller and completely within the domain of attraction of the coexistence equilibrium point E_1. We consider the following model with controls:

$$\begin{cases} dx = \left(rx\left(1 - \dfrac{x}{k}\right) - \dfrac{\beta xy}{a + x^2} + u_1(x, y)\right)dt + \sigma x dB_1, \\ dy = \left(\dfrac{\mu\beta xy}{a + x^2} - dy - \eta xy + u_2(x, y)\right)dt + \sigma y dB_2, \end{cases} \tag{4.1}$$

where $(u_1(x, y), u_2(x, y))^T$ is the control factor and has the following linear form

$$\begin{pmatrix} u_1(x, y) \\ u_2(x, y) \end{pmatrix} = \begin{pmatrix} k_{11} & k_{12} \\ k_{21} & k_{22} \end{pmatrix} \begin{pmatrix} x - \bar{x} \\ y - \bar{y} \end{pmatrix} := K \begin{pmatrix} x - \bar{x} \\ y - \bar{y} \end{pmatrix}.$$

Here, K is the feedback matrix, and $(\bar{x}, \bar{y})$ is the locally stable equilibrium point E_1 of the system (1.1). Next, we will examine the following three control strategies:

$$\begin{aligned} &(1) u_1(x, y) \neq 0, u_2(x, y) \neq 0, \\ &(2) u_1(x, y) \neq 0, u_2(x, y) = 0, \\ &(3) u_1(x, y) = 0, u_2(x, y) \neq 0. \end{aligned}$$

According to the control method in [31], we note that for stochastic systems with added controls

$$dx = f(x, u(x))dt + \epsilon\sigma(x, u(x))d\omega(t),$$

where $f(x, u(x))$ is a sufficiently smooth vector function, ϵ is the scalar parameter of perturbation intensity, $\sigma(x, u(x))$ is a sufficiently smooth $n \times n$ matrix function characterizing the state and control, and $\omega(t)$ is an n-dimensional Wiener process.

Further, the system can be simplified as

$$dz = (A + BK)zdt + \epsilon G d\omega,$$

$$A = \frac{\partial f}{\partial x}(\bar{x}, 0), B = \frac{\partial f}{\partial u}(\bar{x}, 0), G = \sigma(\bar{x}, 0), K = \frac{\partial u}{\partial x}(\bar{x}).$$

The aim of the control is to provide an assigned stochastic sensitivity matrix W by choosing a suitable feedback matrix K, where K satisfies $Re\lambda_i(A + BK) < 0$. The matrix W is the solution of the equation

$$(A + BK)W + W(A + BK)^T + S = 0, S = GG^T.$$

If the rank $B = n$, then for the selected assigned positive definite matrix W, the feedback matrix K is

$$K = -B^{-1}\Big(\frac{1}{2}S W^{-1} + A\Big). \tag{4.2}$$

If the rank $B < n$, the matrix W satisfies the equation

$$P_2(S + AW + WA^T)P_2 = 0, P_1 = BB^+, P_2 = I - P_1, \tag{4.3}$$

where B^+ is the generalized inverse of B. Then the feedback matrix K is

$$K = B^+(S + AW + WA^T)\Big(\frac{1}{2}P_1 - I\Big)W^{-1}. \tag{4.4}$$

We take the parameters in (2.1), $k = 1.45$, $P = 0.95$ and the same noise intensity $\sigma = 0.0175$ as that applied in Figure 3. When we apply Strategy 1), the matrix $B = \begin{pmatrix} 1 & 0 \\ 0 & 1 \end{pmatrix}$; then, we respectively choose the stochastic sensitive matrix and its inverse as

$$W = \begin{pmatrix} 35 & -3 \\ -3 & 0.5 \end{pmatrix}, W^{-1} = \begin{pmatrix} 0.0588 & 0.3529 \\ 0.3529 & 4.1176 \end{pmatrix},$$

which is a symmetric positive definite matrix. Because $rankB = 2$, the feedback matrix is known from (4.2) as

$$K = -B^{-1}\Big(\frac{1}{2}S W^{-1} + A\Big) = \begin{pmatrix} -0.0078 & 0.2469 \\ -0.0096 & -0.0066 \end{pmatrix}.$$

Then, the confidence ellipses of the uncontrolled system (2.2) and the controlled system (4.1) at the equilibrium point E_1 are as indicated by the green line and the blue line in Figure 8(a), respectively. Obviously, the confidence ellipse controlled by Strategy 1) is completely within the domain of attraction of the coexistence equilibrium point E_1. It can be seen in Figure 8(b) that the corresponding time series is maintained around high biomass. Unlike the extinction situation shown in Figure 3, the stochastic model after adopting the control strategy 1) avoids the extinction of predators.

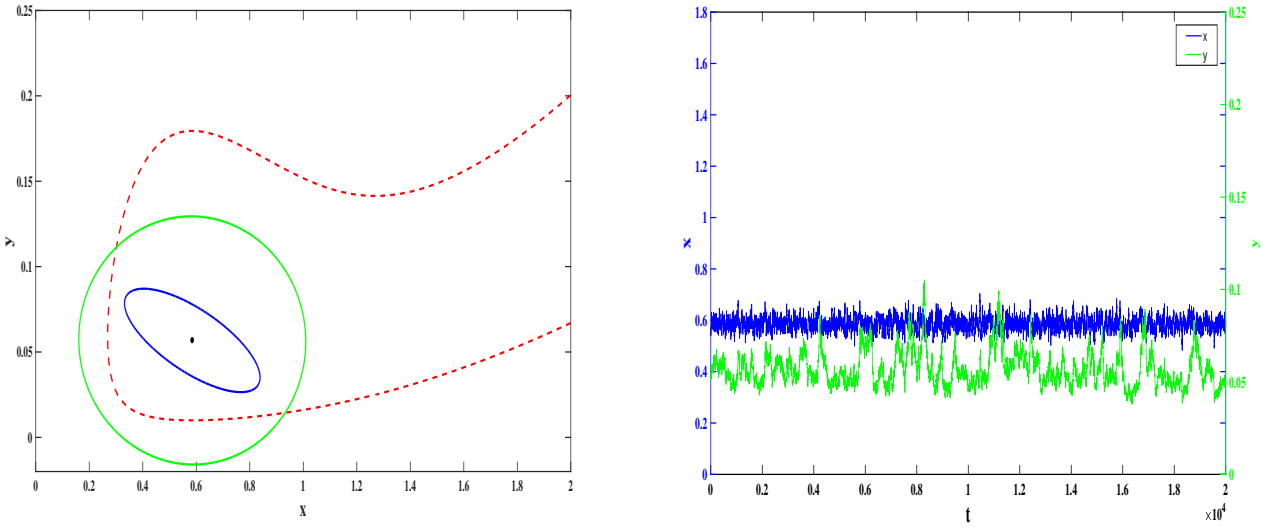

(a) (b)

Figure 8. Confidence ellipses and time series for system (4.1) with control strategy 1). (a) Separatrix (red dotted line) and confidence ellipse (green) of the stochastic model (2.2) without control and with the control strategy 1) (blue) and (b) the time series after adopting the control strategy 1).

When we apply Strategy 2), the matrix $B = \begin{pmatrix} 1 & 0 \\ 0 & 0 \end{pmatrix}$; because $rankB = 1 < 2$, according to $P_1 = BB^+$ and $P_2 = I - P_1$, we have

$$P_1 = \begin{pmatrix} 1 & 0 \\ 0 & 0 \end{pmatrix}, P_2 = \begin{pmatrix} 0 & 0 \\ 0 & 1 \end{pmatrix}.$$

We can respectively assign the stochastic sensitive matrix and its inverse as

$$W = \begin{pmatrix} 3 & -0.1790836 \\ -0.1790836 & 1 \end{pmatrix}, W^{-1} = \begin{pmatrix} 0.3369 & 0.0603 \\ 0.0603 & 1.0108 \end{pmatrix},$$

satisfying (4.3); according to (4.4), the feedback matrix K can be known as

$$K = B^+(S + AW + WA^T)\left(\frac{1}{2}P_1 - I\right)W^{-1} = \begin{pmatrix} -0.0570 & 0.2697 \\ 0 & 0 \end{pmatrix}.$$

Then, the confidence ellipses of the uncontrolled system (2.2) and the controlled system (4.1) at the equilibrium point E_1 are shown as the green line and the blue line in Figure 9(a), respectively. Obviously, the confidence ellipse of the system being controlled by Strategy 2) becomes smaller and completely lies within the attraction domain of the equilibrium point E_1. Similarly, it can also be seen in Figure 9(b) that the corresponding time series is maintained around high biomass. Unlike the extinction situation shown in Figure 3, the stochastic model after adopting the control strategy 2) avoids the extinction of predators.

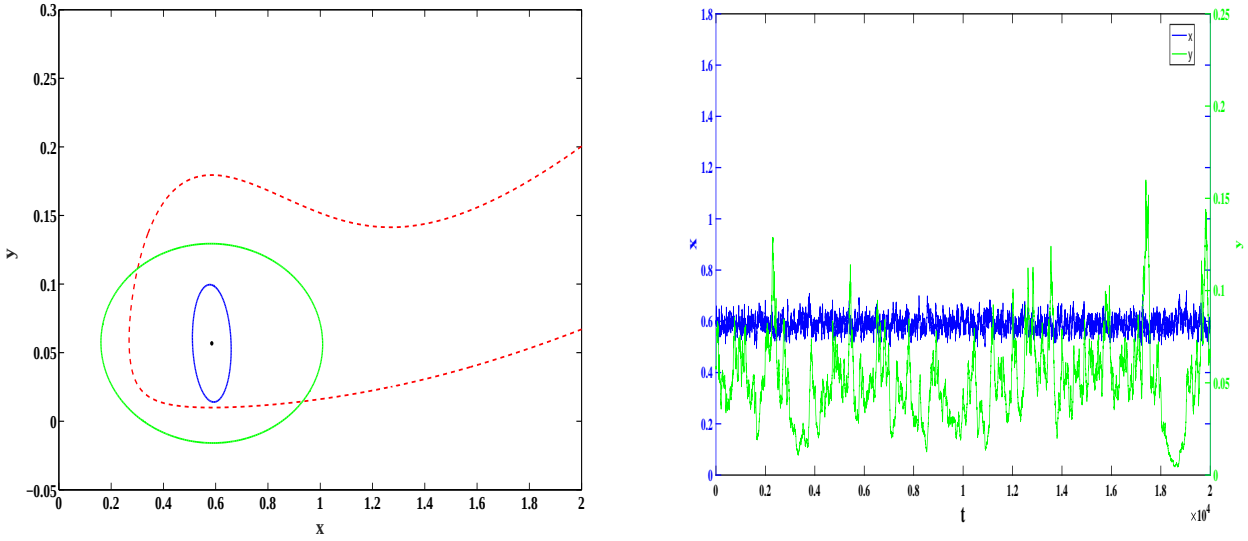

(a) (b)

Figure 9. Confidence ellipses and time series for system (4.1) with control strategy 2). (a) Separatrix (red dotted line) and confidence ellipse (green) of the stochastic model (2.2) without control and the system (4.1) with the controll strategy 2) (blue) and (b) time series after adopting the control strategy 2).

When we apply Strategy 3), the matrix $B = \begin{pmatrix} 0 & 0 \\ 0 & 1 \end{pmatrix}$; because $rankB = 1 < 2$, according to $P_1 = BB^+$ and $P_2 = I - P_1$, we have

$$P_1 = \begin{pmatrix} 0 & 0 \\ 0 & 1 \end{pmatrix}, P_2 = \begin{pmatrix} 1 & 0 \\ 0 & 0 \end{pmatrix}.$$

We can respectively assign the stochastic sensitive matrix and its inverse as

$$W = \begin{pmatrix} 40 & 0.25761521 \\ 0.25761521 & 1 \end{pmatrix}, W^{-1} = \begin{pmatrix} 0.0250 & -0.0065 \\ -0.0065 & 1.0017 \end{pmatrix},$$

satisfying (4.3); then, according to (4.4), the feedback matrix K can be known as

$$K = B^+(S + AW + WA^T)\left(\frac{1}{2}P_1 - I\right)W^{-1} = \begin{pmatrix} 0 & 0 \\ -0.0013 & -0.0036 \end{pmatrix}.$$

The confidence ellipse corresponding to the controlled system (4.1) is shown in Figure 10(a). Similar to the results of adopting Strategy 2), the confidence ellipse becomes smaller and completely lies within the attraction domain of the equilibrium point E_1. It can also be seen in Figure 10(b) that the corresponding time series is maintained around high biomass. Unlike the extinction situation shown in Figure 3, the stochastic model after adopting the control strategy 3) avoids the extinction of predators.

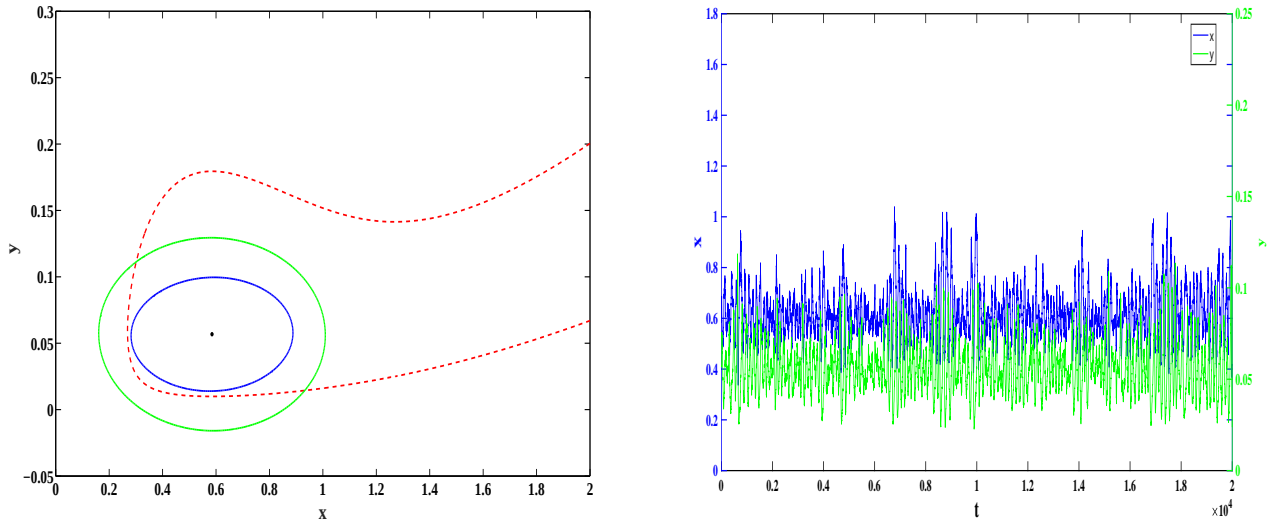

(a) (b)

Figure 10. Confidence ellipses and time series for system (4.1) with control strategy 3). (a) Separatrix (red dotted line), confidence ellipse (green) of the stochastic model (2.2) without control and the system (4.1) with the control strategy 3) (blue) and (b) the time series after adopting the control strategy 3).

4.2. Sensitivity control of coexistence limit cycles

According to the previous analysis, it can be seen that the critical noise intensity for the state transition of the noise-induced system from the stable limit cycle Γ' to the predator extinction equilibrium point E_4 is $\sigma' \approx 0.0094$. Here $\sigma = 0.03 > \sigma'$; the trajectory starting from the vicinity of the limit cycle Γ' finally converges to the predator extinction equilibrium point E_4. To avoid noise-induced transitions from coexistence to extinction, we introduce a feedback control strategy to keep the solution of the system (2.2) in an oscillatory state, and then we consider the following control model similar to model (4.1):

$$\begin{cases} dx = \left(rx\left(1-\dfrac{x}{k}\right) - \dfrac{\beta xy}{a+x^2} + u_3(x,y)\right)dt + \sigma x dB_1, \\ dy = \left(\dfrac{\mu\beta xy}{a+x^2} - dy - \eta xy + u_4(x,y)\right)dt + \sigma y dB_2, \end{cases} \tag{4.5}$$

where we take the parameters in (2.1), $k = 1.6$, $P = 0.95$, and the same noise intensity $\sigma = 0.03$ as that applied in Figure 6. $u_3(x,y)$, $u_4(x,y)$ represent the control function.

According to the control principle in [32], consider a stochastic control system

$$dx = f(x, u(x))dt + \varepsilon\sigma(x, u(x))d\omega(t),$$

where x is the n-dimensional state variable, u is the r-dimensional control function vector, $f(x, u), \sigma(x, u)$ is the vector function, $\omega(t)$ is the n-dimensional Wiener process, and ε is the noise intensity. Assuming $\varepsilon = 0$, $u = 0$, the system has a T-periodic solution $x = \xi(t)$, and the phase diagram trajectory is γ. The feedback control function $u(x)$ satisfies the following conditions:

(a) $u(x)$ is sufficiently smooth and $u|_\gamma = 0$;

(b) The deterministic system is

$$dx = f(x, u(x))dt,$$

and the solution $x = \xi(t)$ is exponentially stable in the neighborhood Γ of the cycle γ. Our aim is to control the stochastic sensitive function W, which satisfies the equation

$$\dot{W} = F(t, u)W + WF^T(t, u) + P(t)S(t)P(t), \tag{4.6}$$

$$F(t, u) = \frac{\partial f}{\partial x}(\xi(t), 0) + \frac{\partial f}{\partial u}(\xi(t), 0)\frac{\partial u}{\partial x}(\xi(t)), S(t) = \sigma(\xi(t), 0)\sigma^T(\xi(t), 0), P(t) = p^T(t)p(t),$$

where $p(t)$ is the normalized orthogonal vector at point $\xi(t)$. It can be seen that controlling u changes only $F(t, u)$, and in fact, the result depends only on the value of the derivative $\dfrac{\partial u}{\partial x}$. Therefore, further consider the Taylor expansion of $u(x)$ at point γ

$$u(x) = u(\gamma) + \frac{\partial u}{\partial x}(\gamma)(x - \gamma) + O(\|x - \gamma\|^3).$$

For $\gamma = \gamma(x)$, using property (a), we get

$$u(x) = \frac{\partial u}{\partial x}(\gamma) \triangle (x) + O(\| \triangle (x)\|^3),$$

where $\triangle(x) = x - \gamma(\mathrm{x})$. It can be approximated as

$$u_1(x) = \Phi(\gamma(x)) \triangle (x),$$

where $\Phi(\gamma(x))$ is the feedback matrix coefficient; denote $K(t) = \Phi(\xi(t))$ and $t(x) = \xi^{-1}(\gamma(x))$; then, we have

$$u = K(t(x)) \triangle (x). \tag{4.7}$$

Therefore, the feedback matrix $K(t)$ completely determines the ability of the regulator $u = K(t(x)) \triangle (x)$ to synthesize $W(t)$.

When controlling for the stochastic sensitivity function of 2D-cycles, let the sensitivity function be μ, and it is the solution of the following boundary value problem

$$\dot{\mu} = a(t)\mu + b(t), \mu(0) = \mu(T), \tag{4.8}$$

$$a(t) = p^T(t)(F^T(t,u) + F(t,u))p(t), b(t) = p^T(t)S(t)p(t).$$

Further, it can be seen that

$$\begin{aligned} a(t) &= a_0(t) + a_1(t), \\ a_0(t) &= 2q^T(t)p(t), \\ a_1(t) &= 2\beta^T(t)k(t), \end{aligned} \tag{4.9}$$

where

$$\begin{aligned} q(t) = A(t)p(t), \beta(t) = B(t)p(t), A(t) = [\frac{\partial f}{\partial x}(\xi(t),0)]^T, \\ B(t) = [\frac{\partial f}{\partial u}(\xi(t),0)]^T, k(t) = \frac{\partial u}{\partial x}(\xi(t))p(t) = K(t)p(t). \end{aligned}$$

According to (4.7), and given $\triangle = P\triangle$, $P = p^T p$, $k = Kp$, we know that

$$u = k(t(x))p^T(t(x)) \triangle (x). \tag{4.10}$$

Then, change the feedback $k(t)$ to construct different stochastic sensitivity functions for the limit cycle. Denote $\bar{\mu}(t)$ as an assignment sensitivity function; then, a cycle γ is completely stochastic controllable if and only if $\beta(t) \neq 0$, $\forall t \in [0,T]$, and the relationship between $\bar{\mu}(t)$ and the control parameter $k(t)$ is

$$\beta^T(t)k(t) = \frac{\bar{a}_1(t)}{2}, \tag{4.11}$$

where

$$\bar{a}_1(t) = \frac{\dot{\bar{\mu}}(t) - a_0(t)\bar{\mu}(t) - b(t)}{\bar{\mu}(t)}.$$

Next, notice the additional optimality criteria

$$\|k(t)\|^2 \to \min.$$

Then the corresponding optimal control has a unique solution

$$\bar{k}(t) = \frac{\bar{a}_1(t)\beta(t)}{2\beta^T(t)\beta(t)} = \frac{(\dot{\bar{\mu}}(t) - a_0(t)\bar{\mu}(t) - b(t))\beta(t)}{2\bar{\mu}(t)\beta^T(t)\beta(t)}, \tag{4.12}$$

and the corresponding Lyapunov exponent λ of the system can be simplified as

$$\lambda = -\frac{1}{2T}\int_0^T \frac{b(t)}{\bar{\mu}(t)}dt.$$

Therefore, for any $\bar{\mu}(t) > 0$, we have $\lambda < 0$. That is to say, the selected sensitive function need only satisfy $\bar{\mu}(t) > 0$.

To avoid the extinction of predators, we exploit the limit cycle sensitivity control principle for the system (4.5) and assign the matrix $B = \begin{pmatrix} 1 & 0 \\ 0 & 1 \end{pmatrix}$ and $\beta(t) \equiv p(t)$. It then follows from (4.11) that

$$\bar{k}(t) = \frac{\bar{a}_1(t)p(t)}{2}, \tag{4.13}$$

which can be simplified to the following form

$$u_3 = \frac{\bar{a}_1(t(x,y))}{2}(x - \xi_1(t(x,y))), \quad u_4 = \frac{\bar{a}_1(t(x,y))}{2}(y - \xi_2(t(x,y))), \tag{4.14}$$

where $\bar{a}_1(t)$ is a scalar function of $\bar{\mu}(t)$ taking the following form:

$$\bar{a}_1(t) = \frac{\dot{\bar{\mu}}(t) - a_0(t)\bar{\mu}(t) - b(t)}{\bar{\mu}(t)},$$

where

$$a_0(t) = \frac{2f_{11}f_2^2 - (f_{12} + f_{21})f_1f_2 + 2f_{22}f_1^2}{f_1^2 + f_2^2}, b(t) = \frac{f_2^2}{f_1^2 + f_2^2},$$
$$f_1 = r\xi_1\left(1 - \frac{\xi_1}{k}\right) - \frac{\beta\xi_1\xi_2}{a + \xi_1^2}, f_2 = \frac{\mu\beta\xi_1\xi_2}{a + \xi_1^2} - d\xi_2 - \eta\xi_1\xi_2,$$
$$f_{11} = r - \frac{2r\xi_1}{k} - \frac{\beta\xi_2}{a + \xi_1^2} + \frac{2\beta\xi_1^2\xi_2}{(a + \xi_1^2)^2}, f_{12} = -\frac{\beta\xi_1}{a + \xi_1^2},$$
$$f_{21} = \frac{\mu\beta\xi_2}{a + \xi_1^2} - \frac{2\mu\beta\xi_1^2\xi_2}{(a + \xi_1^2)^2} - \eta\xi_2, f_{22} = \frac{\mu\beta\xi_1}{a + \xi_1^2 - d - \eta\xi_1},$$

and $\xi_1(t)$, $\xi_2(t)$ are the coordinates of the T periodic vector function $\xi(t) = (\xi_1(t), \xi_2(t))^T$ of the deterministic limit cycle Γ'.

Next, we consider the two parameter control cases of the system (4.5). For the first one, $\sigma = 0.03$ and $\bar{\mu} = 0.8$, the phase diagram of the system (4.5) is shown in Figure 11(a). The red dotted line in this figure is the separatrix of the attraction domain between the deterministic limit cycle Γ' and the predator extinction equilibrium point E_4. The green solid line is the deterministic limit cycle Γ'. The blue line is the trajectory starting from $(0.836, 0.06)$ near the limit cycle after control. Obviously, the controlled stochastic trajectory oscillates near the deterministic limit cycle Γ', and the controlled trajectory is completely inside the attraction domain of the coexistence limit cycle Γ'; its corresponding time series is shown in Figure 11(b). At this time, the solution of the system (4.5) remains oscillatory and the controlled model (4.5) avoids the occurrence of the predator extinction phenomenon in Figure 6.

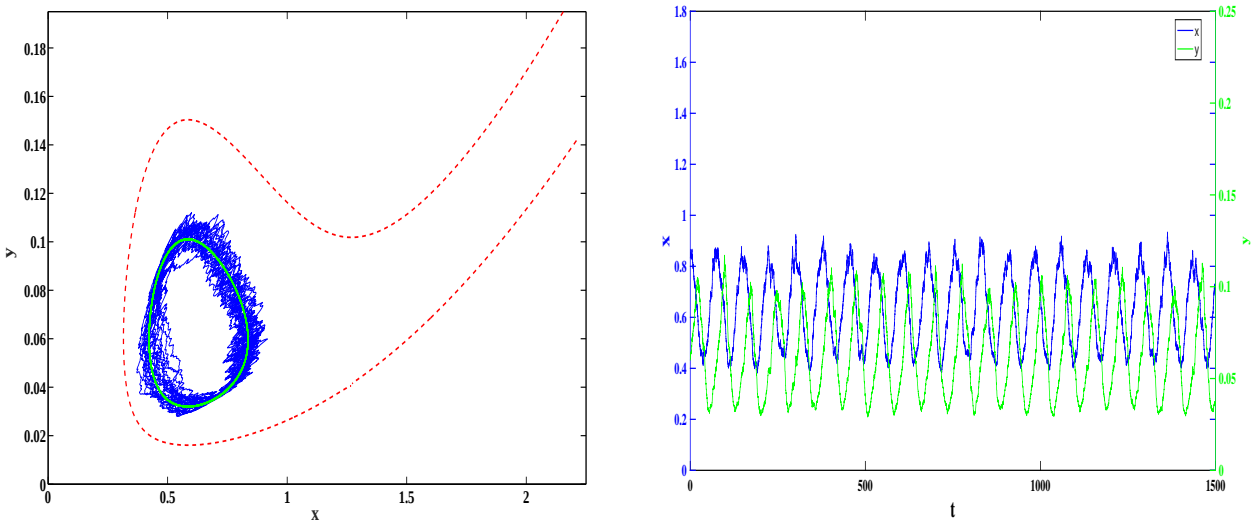

(a) (b)

Figure 11. Trajectory of controlled system (4.5) and corresponding time series. (a) Separatrix (red dotted line), deterministic limit cycle Γ' (green) and random trajectories (blue), and (b) the time series of the controlled system (4.5) with $\sigma = 0.03, \bar{\mu} = 0.8$.

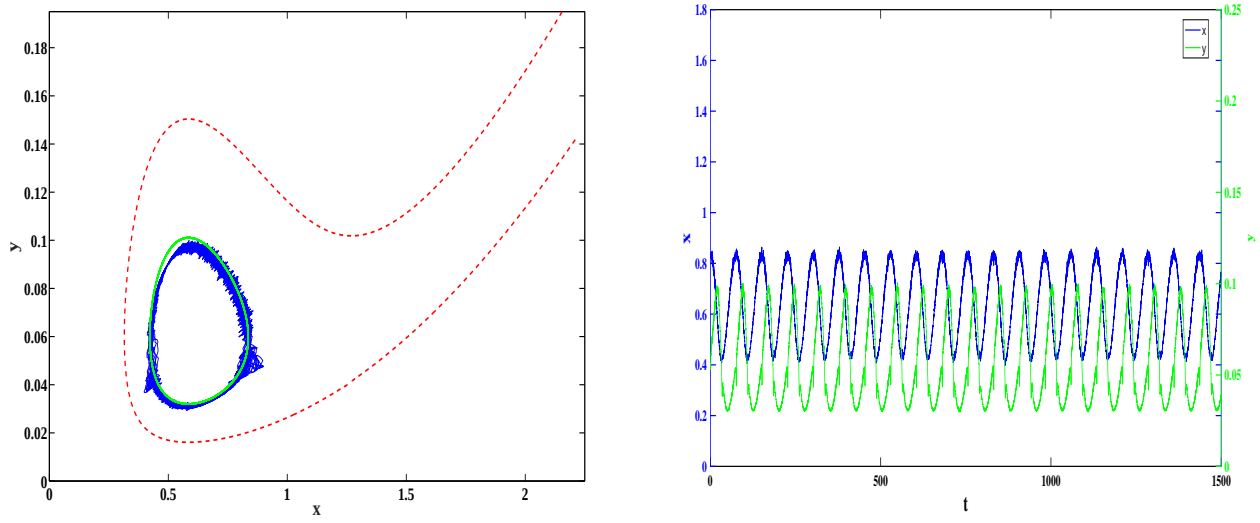

(a) (b)

Figure 12. Trajectory of controlled system (4.5) and corresponding time series. (a) Separatrix (red dotted line), deterministic limit cycle Γ' (green), random trajectories (blue) and (b) the time series of the controlled system (4.5) with $\sigma = 0.03, \bar{\mu} = 0.03$.

Similarly, when $\sigma = 0.03$, $\bar{\mu} = 0.03$, the phase diagram of the system (4.5) is as shown in Figure 12(a). The red dotted line is the separatrix between the two attracting domains, the green solid line is the deterministic limit cycle Γ', and the blue line is a controlled random trajectory starting from

$(0.836, 0.06)$ near Γ'. Obviously, the controlled stochastic trajectory hovers near Γ', but the oscillation amplitude is smaller than that for $\sigma = 0.03$, $\bar{\mu} = 0.8$; the controlled trajectories are all located inside the attraction domain of the deterministic limit cycle Γ'. The solution of the system (4.5) remains oscillatory, and its corresponding time series is shown in Figure 12(b). The controlled model (4.5) avoids the occurrence of the predator extinction phenomenon that can be seen in Figure 6.

According to the two different control results, unlike the predator extinction case shown in Figure 6, both control strategies can keep the solution of the system oscillating. It can also be seen in Figures 11(a) and 12(a) that the control sensitivity can avoid the occurrence of predator extinction, and that, with the decrease of the selected sensitivity function, the magnitude of population fluctuations is reduced.

5. Discussion

In this paper, our focus was on noise-induced transitions from the coexistence state to predator extinction for a stochastic predator-prey model with anti-predator behavior. The corresponding deterministic model has two different bistable states under two different sets of parameters. When $k = 1.45$, as shown in Figure 1(a), the system (1.1) has a stable coexistence equilibrium point $E_1 = (0.58509, 0.05678)$, a saddle point $E_2 = (1.26925, 0.02505)$ and a stable boundary equilibrium point $E_3 = (1.45, 0)$. At this time, the system (1.1) has a bistable point between E_1 and E_3, the stable manifold of E_2 is the separatrix between the two domains of attraction. When $k = 1.6$, as shown in Figure 1(b), the system (1.1) has a stable boundary equilibrium point $E_4 = (1.6, 0)$, a saddle point E_2. At this time, E_1 is unstable, and there is a stable limit cycle Γ', the red dotted line Γ in the figure is the separatrix of two domains of attraction. Obviously, there will be a coexistence area and a predator extinction area in both cases. We found that when the system is affected by a certain degree of environmental noise, the trajectory starting from the coexistence area will cross the separatrix and eventually converges to the predator extinction equilibrium. This is shown in Figures 3 and 6.

In order to estimate the critical threshold of the system state switching under the influence of environmental noise, we used the stochastic sensitive function technique to construct corresponding confidence ellipses or confidence bands for the two cases, respectively. Then, when the confidence ellipse (or the outer boundary of the confidence band) is tangent to the separatrix of two attraction domains, the noise intensity is the estimated value of the critical threshold for the state transition from coexistence to extinction.

When the environmental noise continues to increase, the confidence ellipse and the outer boundary of the confidence band will also become larger, gradually increasing to exceed the separatrix of the two attracting domains and contain part of the attracting domain of the predator extinction equilibrium point. But from a biological point of view, people often prefer species to maintain a high biomass state to enrich the diversity and stability of ecosystems. In order to avoid the occurrence of population extinction, we used two different feedback control methods to control the two situations respectively, and the "solution" of the controlled model was maintained around high biomass.

We mainly used the stochastic sensitivity function technique to find the critical threshold for noise-induced state switching, so as to maintain the biomass near high biomass levels, and we applied two different control strategies to the stochastic model. The system studied in this paper is a two-dimensional predator-prey system, so whether the stochastic sensitive function technique and

feedback control technology used in this paper are suitable for a high-dimensional food chain system still needs further research.

Acknowledgements

The research was supported by the National Natural Science Foundation of China (12071293).

Conflict of interest

The authors declare there is no conflict of interest.

References

1. B. Dubey, Sajan, A. Kumar, Stability switching and chaos in a multiple delayed prey-predator model with fear effect and anti-predator behavior, *Math. Comput. Simul.*, **188** (2021), 164–192. https://doi.org/10.1016/j.matcom.2021.03.037
2. Y. Choh, M. Ignacio, M. W. Sabelis, A. Janssen, Predator-prey role reversals, juvenile experience and adult antipredator behaviour, *Sci. Rep.*, **2** (2012), 1–6. https://doi.org/10.1038/srep00728
3. G. Polis, C. Myers, R. Holt, The ecology and evolution of intraguild predation: Potential competitors that eat each other, *Ann. Rev. Ecol. Syst.*, **20** (1989), 297–330. https://doi.org/10.1146/annurev.es.20.110189.001501
4. S. Kumar, T. Yasuhiro, Dynamics of a predator-prey system with fear and group defense, *J. Math. Anal. Appl.*, **481** (2020), 123471–123494. https://doi.org/10.1016/j.jmaa.2019.123471
5. J. Huang, X. Xia, X. Zhang, S. Ruan, Bifurcation of codimension 3 in a predator-Prey system of leslie type with simplified holling type IV functional response, *Int. J. Bifurcation Chaos*, **26** (2016). https://doi.org/10.1142/S0218127416500346
6. R. Yang, J. Ma, Analysis of a diffusive predator-prey system with anti-predator behaviour and maturation delay, *Chaos Solitons Fractals*, **109** (2018), 128–139. https://doi.org/10.1016/j.chaos.2018.02.006
7. C. Li, H. Zhu, Canard cycles for predator-prey systems with Holling types of functional response, *J. Differ. Equations*, **254** (2013). https://doi.org/10.1016/j.jde.2012.10.003
8. D. Xiao, S. Ruan, Global analysis in a predator-prey system with nonmonotonic functional response, *SIAM J. Appl. Math.*, **61** (2000), 1445–1472. https://doi.org/10.1137/S0036139999361896
9. D. Xiao, S. Ruan, Multiple bifurcations in a delayed predator-prey system with nonmonotonic functional response, *J. Differ. Equations*, **176** (2001), 494–510. https://doi.org/10.1006/jdeq.2000.3982
10. H. Zhu, S. A. Campbell, G. S. K. Wolkowicz, Bifurcation analysis of a predator-prey system with nonmonotonic functional response, *SIAM J. Appl. Math.*, **63** (2003), 636–647. https://doi.org/10.1137/S0036139901397285

11. B. Tang, Y. Xiao, Bifurcation analysis of a predator-prey model with anti-predator behaviour, *Chaos Solitons Fractals*, **70** (2015), 58–68. https://doi.org/10.1016/j.chaos.2014.11.008
12. S. Zhang, S. Yuan, T. Zhang, Dynamic analysis of a stochastic eco-epidemiological model with disease in predators, *Stud. Appl. Math.*, **149** (2021), 5–42. https://doi.org/10.1111/sapm.12489
13. C. Xu, S. Yuan, T. Zhang, Competitive exclusion in a general multi-species chemostat model with stochastic perturbations, *Bull. Math. Biol.*, **83** (2021). https://doi.org/10.1007/s11538-020-00843-7
14. J. Yang, S. Yuan, Dynamics of a toxic producing phytoplankton-zooplankton model with three-dimensional patch, *Appl. Math. Lett.*, **118** (2021), 107146. https://doi.org/10.1016/j.aml.2021.107146
15. A. Yang, B. Song, S. Yuan, Noise-induced transitions in a non-smooth SIS epidemic model with media alert, *Math. Biosci. Eng.*, **18** (2020), 745–763. https://doi.org/10.3934/mbe.2021040
16. Q. Yang, X. Zhang, D. Jiang, M. Shao, Analysis of a stochastic predator-prey model with weak Allee effect and Holling-(n+1) functional response, *Commun. Nonlinear Sci. Numer. Simul.*, **111** (2022). https://doi.org/10.1016/j.cnsns.2022.106454
17. T. Zhang, X. Liu, X. Meng, T. Zhang, Spatio-temporal dynamics near the steady state of a planktonic system, *Comput. Math. Appl.*, **75** (2018), 4490–4504. https://doi.org/10.1016/j.camwa.2018.03.044
18. S. A. Bawa, P. C. Gregg, A. P. Del Socorro, C. Miller, N. R. Andrew, Exposure of Helicoverpa punctigera pupae to extreme temperatures for extended periods negatively impacts on adult population dynamics and reproductive output, *J. Therm. Biol.*, **101** (2021). https://doi.org/10.1016/j.jtherbio.2021.103099
19. C. Kurrer, K. Schulten, Effect of noise and perturbations on limit cycle systems, *Phys. D Nonlinear Phenom.*, **50** (1991), 311–320. https://doi.org/10.1016/0167-2789(91)90001-P
20. F. Gassmann, Noise-induced chaos-order transitions, *Phys. Rev. E*, **55** (1997), 2215–2221. https://doi.org/10.1103/PhysRevE.55.2215
21. S. Kraut, U. Feudel, Multistability, noise and attractor-hopping: The crucial role of chaotic saddles, *Phys. Rev. E*, **66** (2002), 015207. https://doi.org/10.1103/PhysRevE.66.015207
22. J. B. Gao, S. K. Hwang, J. M. Liu, When can noise induce chaos?, *Phys. Rev. Lett.*, **82** (1999), 1132–1135. https://doi.org/10.1103/PhysRevLett.82.1132
23. Q. Liu, D. Jiang, T. Hayat, A. Alsaedi, Stationary distribution of a regime-switching predator-prey model with anti-predator behaviour and higher-order perturbations, *Phys. A*, **515** (2019), 199–210. https://doi.org/10.1016/j.physa.2018.09.168
24. S. Zhang, S. Yuan, T. Zhang, A predator-prey model with different response functions to juvenile and adult prey in deterministic and stochastic environments, *Appl. Math. Comput.*, **413** (2022), 126598. https://doi.org/10.1016/j.amc.2021.126598
25. B. Zhou, B. Han, D. Jiang, T. Hayat, A. Alsaedi, Stationary distribution, extinction and probability density function of a stochastic vegetation-water model in arid ecosystems, *J. Nonlinear Sci.*, **32** (2022). https://doi.org/10.1007/s00332-022-09789-7

26. Q. Yang, X. Zhang, D. Jiang, Dynamical behaviors of a stochastic food chain system with ornstein-uhlenbeck process, *J. Nonlinear Sci.*, **32** (2022). https://doi.org/10.1007/s00332-022-09796-8

27. Z. Shi, D. Jiang, X. Zhang, A. Alsaedi, A stochastic SEIRS rabies model with population dispersal: Stationary distribution and probability density function, *Appl. Math. Comput.*, **427** (2022), 427. https://doi.org/10.1016/j.amc.2022.127189

28. Z. Shi, D. Jiang, Dynamical behaviors of a stochastic HTLV-I infection model with general infection form and ornstein-uhlenbeck process, *Chaos Solitons Fractals*, **165** (2022). https://doi.org/10.1016/j.chaos.2022.112789

29. I. Bashkirtseva, L. Ryashko, I. Tsvetkov, Sensitivity analysis of stochastic equilibria and cycles for the discrete dynamic systems, *Dyn. Contin. Discrete Impulsive Syst.*, **17** (2010), 501–515.

30. S. Yuan, D. Wu, G. Lan, H. Wang, Noise-induced transitions in a nonsmooth producer-grazer model with stoichiometric constraints, *Bull. Math. Biol.*, **82** (2020), 1–22. https://doi.org/10.1007/s11538-020-00733-y

31. L. Ryashko, I. Bashkirtseva, On control of stochastic sensitivity, *Autom. Remote Control*, **69** (2008), 1171–1180. https://doi.org/10.1134/S0005117908070084

32. I. Bashkirtseva, L. Ryashko, Sensitivity and chaos control for the forced nonlinear oscillations, *Chaos Solitons Fractals*, **26** (2005), 1437–1451. https://doi.org/10.1016/j.chaos.2005.03.029

33. I. Bashkirtseva, T. Ryazanova, L. Ryashko, Confidence domains in the analysis of noise-induced transition to chaos for Goodwin model of business cycles, *Int. J. Bifurcation Chaos*, **24** (2014), 1437–1447. https://doi.org/10.1142/S0218127414400203

AIMS Press